Volume Data Mining Using 3D Field Topology Analysis*

Issei Fujishiro[1,3] Taeko Azuma[2] Yuriko Takeshima[2,3] Shigeo Takahashi[4]

1) Department of Information Sciences, Ochanomizu University
2) Graduate School of Humanities and Sciences, Ochanomizu University
3) Research Organization for Information Science & Technology
4) Computer Center, Gunma University

Abstract

This paper takes advantage of a 3D field topology analysis for automating visualization design aiming at volume data mining. The conventional Reeb graph-based approach to describe the topological features of 3D surfaces is extended to capture the topological skeleton of a volumetric field. Based on the analysis results, which are represented in the form of hyper Reeb graph, we propose two methods for effective geometric object fitting and two principles to design appropriate color/opacity transfer functions for direct volume rendering. Feasibility study of the present methodology is performed with a large scale 4D simulated dataset from atomic collision research.

Keywords: Volume visualization, visual data mining, comprehensible rendering, transfer function, isosurface, Reeb graph.

1 Introduction

Volume visualization has served as an indispensable tool to explore the inner structures and complex behavior of volumetric objects embedded in large-scale sampled or simulated 3D datasets. However, the rapid increase in data size makes it difficult for us to sufficiently adjust visualization-related parameters for generating informative images. Those representative parameters include the target level for isosurfacing and transfer functions for direct volume rendering. In order to compensate the lack of interactivity, and to provide the user with the *serendipity*[7], an auxiliary mechanism must be developed, which chooses appropriate values for the visualization parameters based on some available quantitative properties of a given volume dataset.

This paper proposes a novel approach to automating the settings of visualization parameter values for volume data mining. To this end, the conventional Reeb graph-based approach to topological modeling of 3D surfaces [1, 2] is extended to capture the topological skeleton of a volumetric field. The analyzed results are represented in the form of *hyper Reeb graph*[3], which gives the basic reference structure for designing comprehensible volume visualization.

The remainder of this paper is organized as follows. The next section gives an overview of Reeb graph, and describes how we extend the concept to construct a hyper Reeb graph from a given volume. Section 3 delineates two methods for effective geometric object fitting and two design principles for appropriate hue/opacity transfer functions. In Section 4, the implementation aspect of the methodology is focused on. Then we apply the present methodology to visualizing a large scale 4D simulated dataset from atomic collision research in Section 5. Finally, we discuss the extensibility of the methodology, and address related future issues in Section 6.

2 Representing Volume Field Topology

2.1 Reeb graph

Reeb graph has recently been used as a tool for analyzing 3D surface topology in terms of splitting and merging of equi-height contours [1, 2]. Let hf be a height function of a target surface, and let p and q be points on the surface. The Reeb graph of the height function hf is obtained by identifying p and q, if the two points are contained in the same connected component on the cross-section of the surface at the height $hf(p)(= hf(q))$. When using Reeb graph, any surface can be characterized topologically with its nodes which represent either of three kinds of critical points, i.e., *peak*, *pass*, and *pit*, and which are connected to each other by an edge for a set of topologically-equivalent connected contours on consecutive cross-sections. Figure 1 shows two kinds of simple surfaces, ellipsoid and torus, and their corresponding Reeb graphs. Note that as for the torus, altering directions of axis for defining the height function may give different Reeb graphs. In other words, Reeb graph is an unambiguous, but non-unique representation of the surface topology. For the precise definition of Reeb graph, see [1].

*An revised version of this paper is to be published in *IEEE CG & A*, Vol.20, No.5, September/October 2000.

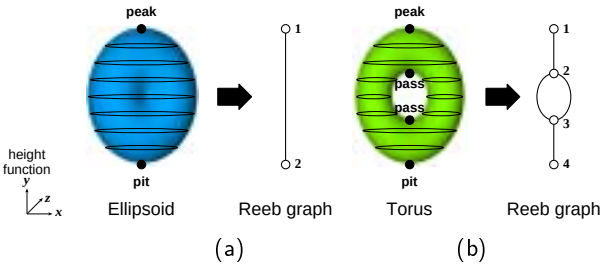

Figure 1: Reeb graphs for simple 3D surfaces. (a) Ellipsoid; (b) Torus.

2.2 Hyper Reeb graph

Hyper Reeb graph (*HRG* for short hereafter) is an extension of the Reeb graph concept to 3D volume fields [3]. Theoretically, a volume can be decomposed into an infinite number of isosurfaces with different target values. The topological feature of each isosurface can be captured by using the Reeb graph with a common definition of height function. Therefore, by examining the sequence of isosurfaces in terms of the structure of Reeb graphs, we can find a particular field value, termed *critical field value* (*CFV*), on which the topological equivalence of consecutive isosurfaces is broken. HRG is a hierarchical graph consisting of two layers of topological data specification. The top layer of the graph is a linear directed graph connecting in an ascending order, m nodes v_i with CFVs $f_i (i = 1, ..., m)$ and two boundary nodes v_0 and v_{m+1} with minimum and maximum field values f_0 and f_{m+1}, respectively. Each edge $e(v_i, v_{i+1})$ retains as its weight, the corresponding topologically-equivalent Reeb graph at the bottom layer as well as the length of the field interval $l_{i,i+1}$ $(= f_{i+1} - f_i)$. Note that if the field interval is open (closed), its boundary nodes are depicted with a void (solid) circle.

As a running example, let us consider the following analytical volume:

$$\begin{aligned} f(x,y,z) &= a^2 + b^2 \\ a &= exp(-\sqrt{x^2+y^2+z^2+1-2\sqrt{x^2+y^2}}) \\ b &= exp(-\sqrt{x^2+y^2+z^2+1+2\sqrt{x^2+y^2}}) \end{aligned}$$

A simple arithmetic shows that the volume, which is called *metatorus* hereafter, has a single CFV $f_1 (= 2e^{-2})$ when and only when $a = b$. Figure 2 illustrates how we construct the HRG for the volume. From the resulting HRG we observe that:

- As the field value increases, ellipsoidal isosurfaces get diminished, and crushed in the direction of the x-axis. Then as passing by the CFV, a single hole appears around the origin, to generate the sequence of nested tori.
- As the field value increases further, the diameter of the rounded tube of the tori becomes smaller.

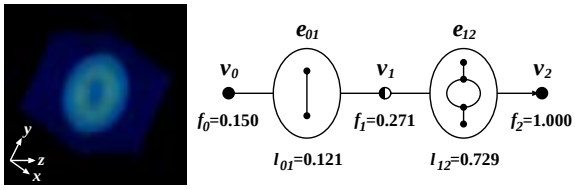

Figure 2: Constructing HRG for *metatorus* volume.

3 Comprehensible Volume Visualization

Now we attempt to take advantage of the HRG-based volumetric field topology description in order to sophisticate the conventional volume visualization techniques.

3.1 Geometric object fitting

We consider the following two options:

- **Method 1:** Simultaneous display of $m + 1$ semi-transparent isosurfaces, each of which is extracted with a field value $(f_i + f_{i+1})/2$ at the midpoint of topologically-equivalent field interval $[f_i, f_{i+1}]$ $(i = 0, ..., m)$. We can determine a plausible value for the opacity of each isosurface so as to reflect the mutual relationships among $l_{i,i+1}$ $(i = 0, ..., m)$ in order to allow us to understand the relative *thickness* of topologically-equivalent field intervals.
- **Method 2:** Decomposing a given volume V disjointly into a sequence of $m + 1$ interval volumes $IV(f_i, f_{i+1})$ $(i = 0, ..., m)$; *i.e.*, $V = \bigcup_{i=0}^{m} IV(f_i, f_{i+1})$. *Interval volume* was proposed in [4] as a solid data representation of 3D subvolume for which the associated field value lie within a specified closed field interval. Topologically-equivalence gives the rigid basis for the volume decomposition. In addition, the boundaries of each interval volume convey informative shape of isosurfaces with CFVs, where the topology of level surfaces exactly changes.

Figure 3 visualizes the *metatorus* volume with the above two methods in a comprehensible manner. The selected isosurfaces in Figure 3(a) can also be utilized as an effective set of basic frames for the *flip book* approach to volume rendering. On the other hand, the set of interval volumes in Figure 3(b) is expected to serve as a good initial step for more sophisticated volume segmentation.

3.2 Transfer function design

It is well-known that one of the most significant factors for determining the quality of volume rendered images is transfer functions, which map physical fields of a given volume dataset to optical properties, such as color and opacity. There are several previous research results on

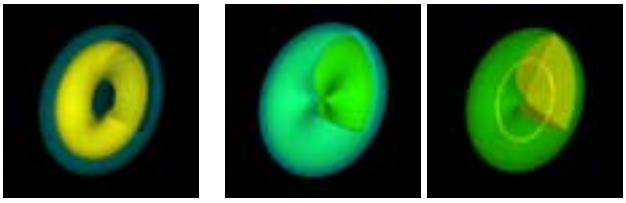

(a) (b)

Figure 3: Geometric object extraction from *metatorus* volume based on HRG in Figure 2. The upper-right-front octant of volume is cropped. (a) Simultaneous display of two isosurfaces with 0.21 (ellipsoid) and 0.64 (torus); (b) Decomposition into two interval volumes $IV[0.15, 0.271]$ and $IV[0.271, 1.0]$.

(semi-)automating transfer function design for informative volume rendering, which are bisected into the two major categories, *image-guided* (e.g., [9, 10]) or *input volume content-based* (e.g., [13, 11, 12]). The approach presented herein can be regarded as a novel one in this second category.

The basic idea of designing appropriate transfer functions based on HRG is to accentuate the topological change in volume fields around CFVs in terms of both color (hue) and opacity. We will specify the two transfer functions within the analyzed subdomain $[f_0, f_{m+1}]$. Hue and opacity transfer functions are set to be *undefined* and 0 (fully transparent) outside of the subdomain, respectively (see Figure 4).

The following two design principles are considered:

- **Principle 1:** The color transfer function is designed so that the change in hue is uniform with respect to field value, except for a constant jump δ_h at each CFV f_i $(i = 1, ..., m)$. On the other hand, the opacity transfer function is designed to be a constant $\alpha(> 0)$, except for a common hat-like small elevation around each CFV f_i $(i = 1, ..., m)$, whose height and width are δ_o and ω_o, respectively (Figure 4(a)).

- **Principle 2:** The hue transfer function is designed to be stepwise elevated at a constant rate δ_h, except for the linear change within a small interval of length ω_h around CFV f_i $(i = 1, ..., m)$. On the other hand, the opacity transfer function is designed to have small constant elevation δ_o relative to the base height α within the same interval of length $\omega_o (= \omega_h)$ around CFV f_i $(i = 1, ..., m)$ (Figure 4(b)).

Figure 5 compares volume rendered images of the *metatorus* volume with the two different designs of transfer functions. The transfer functions designed according to the principle 1 are useful for visually grasping topologically-equivalent interval volumes. On the other hand, the transfer functions designed according to the principle 2 are beneficial for observing the change in topological structures near CFVs in detail. In addition, this

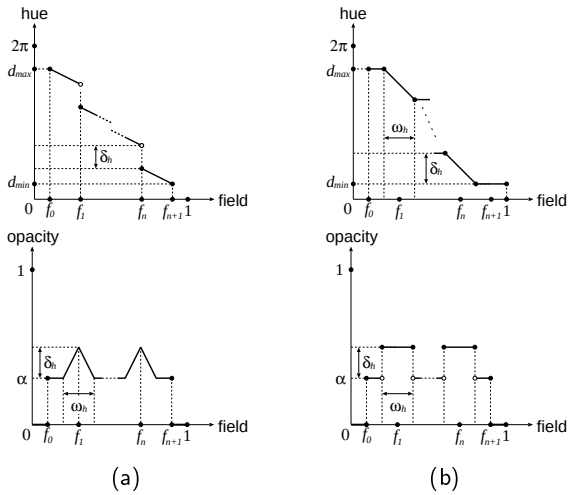

(a) (b)

Figure 4: Design principles of transfer function accentuation. (a) Principle 1; (b) Principle 2.

principle is suitable for the bisection search for CFVs in the digital settings (see Section 4), because in general, a CFV is likely to be specified as an internal point belonging to an field interval of the minimum length.

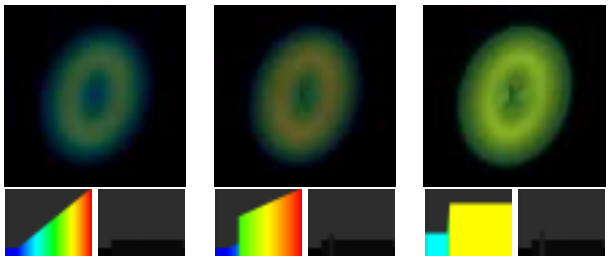

(a) (b) (c)

Figure 5: Volume rendering of *metatorus* with accentuated transfer functions. (a) Using continuous hue and flat opacity transfer functions (reference); (b) Using accentuated transfer functions according to principle 1 ($\delta_h = 2/3\pi; \alpha = 0.02; \delta_o = 0.06; \omega_o = 0.04$); (c) Using accentuated transfer functions according to principle 2 ($\delta_h = 2/3\pi; \alpha = 0.02; \delta_o = 0.06; \omega_h = \omega_o = 0.03$).

4 Implementation

In order to make the present volume data mining methodology applicable to practical sampled or simulated datasets, we have developed a pilot environment on the visualization software platform AVS/Express version 5.0[8][1] running on an SGI O2 system (CPU: R5000, Clock: 180MHz, RAM: 192MB). All the experiments throughout the paper were performed in the same environment.

[1] AVS is a trademark of Advanced Visual Systems, Inc.

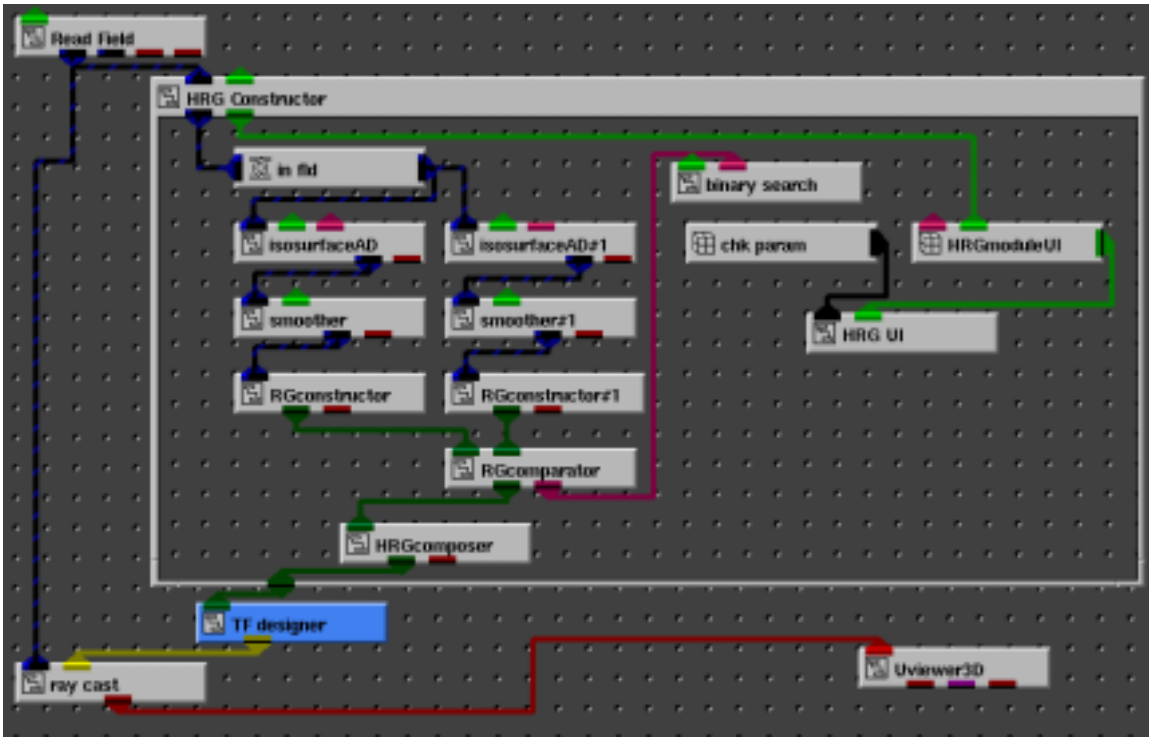

Figure 6: AVS/Express module network for volume data mining.

Figure 6 shows a typical AVS/Express module network used for volume data mining. The HRG constructor is our main proprietary module, which inputs a scalar volume and the axis direction for height function, and generates the corresponding HRG. Isosurfacing is performed using an extended version of the well-known *Marching Cubes* algorithm, which is combined with an auxiliary algorithm, called *Asymptotic Decider*, for maintaining the topological consistency in triangle patch connection. In order to reduce the large number of critical points, due to high frequency components which are likely to appear on an isosurface extracted from practical volume datasets, we adopt a Gaussian-type surface low-pass filter algorithm described in [5]. The Reeb graph of each isosurface is then constructed by a robust algorithm, described in [2], which first extracts all the critical points on a surface whose topology is equivalent with that of sphere or torus correctly in the sense of the Euler formula, then construct the surface network by tracing ridge and ravine lines, and finally convert the surface network to the corresponding Reeb graph. The HRG constructor module employ a bisection-based method to find all the CFVs in the user-specified field interval $[f_0, f_{m+1}]$. To judge the homogeneity of Reeb graphs, we compute two characteristic quantities of the graph, namely, sums of absolute coefficients of characteristic and distance polynomials [6].

The TF designer module takes the HRG structures as its input, and provides accentuated transfer function look-up tables for the in-house ray cast module for a standard volume ray-casting.

5 Application: Proton – Hydrogen Atom Collision

To illustrate the feasibility of the present methodology, we attempt to explore a large-scale 4D dataset, which comprises 10^4 time steps of 61^3 volumes for simulated intermediate energy collision of proton and hydrogen atom [4]. The simulation deals with a fundamental ion-atom collision problem, and is very important in that the problem has a wide spectrum of applications such as nuclear fusion, material sciences and radiology. The purpose here is to investigate how the positive charge of an incident proton affects the behavior of an electron around the target hydrogen atom (Figure 7). To this end, we will get a comprehensible illustration of the collision by visualizing the 3D distorted electron density distribution.

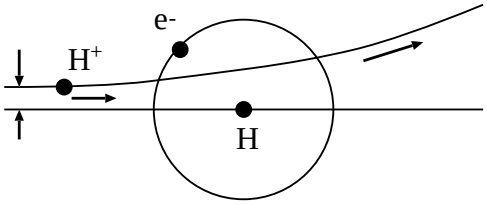

Figure 7: The problem of proton–hydrogen atom collision.

Without producing volume rendered animation of the entire time sequence, we can easily identify an approximate timing of the collision by sampling snapshot volumes and searching the simplest structure among con-

structed HRGs. It is because the stationary electron density distribution around a hydrogen atom constitutes a completely-layered structure of spherical isosurfaces.

Figure 8 depicts three representative snapshots before, around, and after the collision by HRGs; isodensity surfaces extracted with a common target value throughout the entire time interval; and volume rendering instantaneously accentuated according to Principle 2 in Section 3.2. The three types of volume viewings allow us to understand more clearly the inner structures of distorted electron density distribution.

6 Concluding Remarks

This paper has presented a 3D field topology analysis-based methodology for volume data mining. Combined use of the sophisticated indirect/direct volume visualization with HRGs provides the user with effective visual cues for discovering the knowledge about the inner structure and complex behavior of volumetric objects.

The present methodology is quite general; it can be re-combined with the forward approaches to volume rendering, such as splatting and cell projection. Moreover, the methodology is independent of the mesh type of an input volume dataset, as far as a sequence of isosurfaces can be extracted from the dataset.

On the other hand, the current implementaiton of HRG constructor is very sensitive to the change in topology on volume boundaries, and thus making narrower the analyzable field interval $[f_0, f_{m+1}]$. An algorithm to extract a substantial subgraph from a given Reeb graph needs to be developed. In addition, it is crucial to choose an optimal direction for defining height field functions to adjust the viewing direction as well. Omni-directional (spherical) mapping is considered to be one of the convincing solutions to this problem, at the sacrifice of its high temporal complexity.

Furthermore, prioritizing CFVs to control the LOD of HRGs is viewed as the key to breed the present methodology to a true volume data mining tool for various disciplines, including medical sciences and environmental sciences. Candidates for promising strategies include perturbation analysis of the direction for height function axis and relaxation of topological equivalence of Reeb graphs.

Acknowledgements

We have benefited from continuous discussions with Xiaoyang Mao, Yoshihisa Shinagawa, Haruo Hosoya, Koji Koyamada, and research staff from Monolith, Inc. This work has been partially supported by the Ministry of Education, Science, Sports, and Culture, the Japanese government under Grant-in-Aid for Scientific Research (C), 11680349.

References

[1] Y. Shinagawa and T.L. Kunii, "Constructing a Reeb Graph Automatically from Cross Sections," *IEEE Computer Graphics and Applications*, Vol. 11, No. 6, November/December 1991, pp. 44–51.

[2] S. Takahashi, T. Ikeda, Y. Shinagawa, T.L. Kunii, and M. Ueda, "Algorithms for Extracting Correct Critical Points and Constructing Topological Graphs from Discrete Geographical Elevation Data," *Computer Graphics Forum*, Vol. 14, No. 3, August–September 1995, pp. 181–192.

[3] I. Fujishiro, T. Azuma, and Y. Takeshima, "Automating Transfer Function Design for Comprehensible Volume Rendering Based on 3D Field Topology Analysis," In *Proc. IEEE Visualization'99*, ACM Press, New York, NY, October 1999, pp. 467–470, p. 563.

[4] I. Fujishiro, Y. Maeda, H. Sato, and Y. Takeshima, "Volumetric Data Exploration Using Interval Volume," *IEEE Transactions on Visualization and Computer Graphics*, Vol. 2, No. 2, June 1996, pp. 144–155.

[5] G. Taubin, "A Signal Processing Approach to Fair Surface Design," *Computer Graphics* Proceedings, Annual Conference Series, August 1995, ACM SIGGRAPH, pp. 351–358.

[6] L.B. Kier and L.H. Hall, *Molecular Connectivity in Chemistry and Drug Research*, Academic Press, 1976.

[7] N. Ramakrishnan and A. Y. Grama, "Data Mining: From Serendipity to Science," *IEEE Computer* Vol. 32, No 8, pp. 34–37, August 1999.

[8] H. D. Lord, "Improving the Application Visualization Development Process with Modular Visualization Environments," *ACM Computer Graphics*, Vol. 29, No. 2, pp. 9–12, May 1995.

[9] T. He, L. Hong, A. Kaufman, and H. Pfister, "Generation of Transfer Functions with Stochastic Search Techniques," In *Proc. IEEE Visualization '96*, ACM Press, New York, NY, October 1996, pp. 227–234, p. 489.

[10] J. Marks, et al., "Design Galleries: A General Approach to Setting Parameters for Computer Graphics and Animation," In *Computer Graphics Proceedings, Annual Conference Series*, ACM SIGGRAPH, August 1997, pp. 389–400.

[11] G. Kindlmann and J. W. Durkin, "Semi-Automatic Generation of Transfer Functions for Direct Volume Rendering," In *Proc. IEEE Symposium on Volume Visualization*, ACM SIGGRAPH, October 1998, pp. 79–86, p. 170.

[12] S. Fang, T. Biddlecome, and M. Tuceryan, "Image-Based Transfer Function Design for Data Exploration," In *Proc. IEEE Visualization'98*, ACM Press, New York, NY, October 1998, pp. 319–326, p. 546.

[13] S. Castro, A. Koenig, H. Loeffelmann, and E. Groeller: "Transfer Function Specification for the Visualization of Medical Data," Technical Report, Vienna University of Technology, TR–186–2–98–12, March 1998.

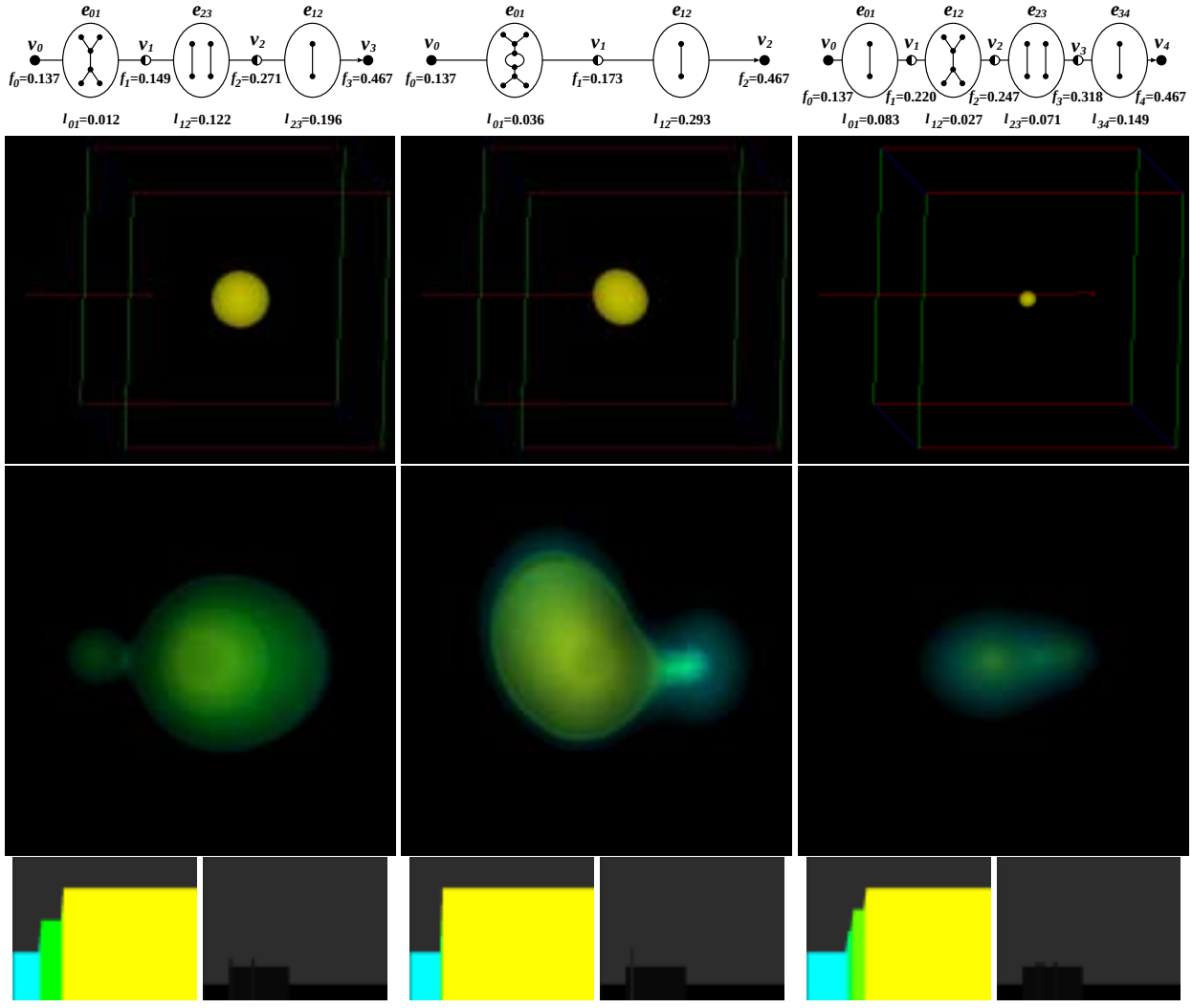

(a) (b) (c)

Figure 8: Three types of volume data mining snapshots of proton–hydrogen atom collision: HRG (top); isodensity surface with the trajectory of marching proton (middle); and accentuated volume rendering (bottom). (a) Before collision; (b) Around collision; and (c) After collision.